

Experimental observation of an intrinsic instability toward multiple-gap states in nonequilibrium superconducting aluminum films by high quasiparticle injection

I. Iguchi

Institute of Materials Science, University of Tsukuba, Sakura-mura, Ibaraki-ken 305, Japan

D. Kent, H. Gilmartin, and D. N. Langenberg

Department of Physics and Laboratory for Research on the Structure of Matter,

University of Pennsylvania, Philadelphia, Pennsylvania 19104

(Received 17 November 1980)

Measurements are reported of the inhomogeneous gap states in a superconducting Al film driven far from thermal equilibrium by tunnel injection using Pb/Bi-I-Al(2)-I-Al(1) double-tunnel junctions in which the gap parameter $\Delta_{\text{Al}(2)}$ is appreciably smaller than $\Delta_{\text{Al}(1)}$. Quasiparticles are injected in the middle Al(2) film by a Pb/Bi-I-Al(2) injector. Above a certain threshold current, an intrinsic instability is observed, followed by the development of distinct gap states. For injection at the gap-sum voltage of the injector characteristic, we observe a two-gap state similar to previous observations, while for injection above the gap-sum voltage, we observe the subsequent appearance of the multiple-gap regions at a series of threshold currents. The results are consistently interpreted by an instability model developed based on the Scalapino-Huberman model.

I. INTRODUCTION

It is well known that there are many nonlinear systems which exhibit instabilities against fluctuations in the uniform steady state when the systems are driven far from thermodynamic equilibrium. Such examples are hydrodynamic instabilities, laser instabilities, some biological instabilities and so on.¹ The instability which occurs in a superconducting film under high quasiparticle injection may be also considered to be one of such kind of instability. As a consequence of fluctuations, the instability leads to either a second-order or first-order phase transition and new types of structures may appear. The possible establishment of spatially inhomogeneous states has so far been reported under the conditions of optical irradiation and tunnel injection of quasiparticles, although the possibility of time-varying states may not be excluded. The experimental results suggest that the resultant inhomogeneous state will be a mixed state of normal and superconducting regions, a mixed state of distinct gap regions, or a smoothly varying gap state, depending on the qualitative natures of the injection source, sample materials, and sample surroundings (i.e., the acoustic matching at the boundary surface).

For tin films, a partial resistive state² and considerable gap broadening in the IV characteristics³ under laser irradiation, as well as instability toward the inhomogeneous gap state under tunnel injection⁴ have been observed. For lead films, in addition to the partial resistive state⁵⁻⁷ and the instability toward the in-

homogeneous gap state,⁸ a first-order transition to the normal state was also observed below T_λ under tunnel injection^{8,9} or phonon injection experiments.¹⁰ In the case of aluminum films, an experiment using laser irradiation has been reported.¹¹ For tunnel injection, the recent experiments by Dynes, Narayanamurti, and Garno (DNG),¹² and Gray and Willemssen (GW)¹³ demonstrated the appearance of the distinct gap states. DNG pointed out that their observation could not be explained by trivial effects such as simple heating or critical current instability and was the result of an intrinsic instability in the superconductor. On the other hand, GW interpreted their results by a less physically interesting load-line switching model based on small spatial inhomogeneities in the films and the extremely nonlinear IV characteristics.^{13,14}

Several theoretical models¹⁵⁻²⁴ have been proposed to investigate the stability of the nonequilibrium state of superconductors. For example, Owen and Scalapino¹⁵ studied the thermodynamic instability by assuming the special μ^* distribution of quasiparticles (the μ^* model). The instability led to a first-order transition to the normal state in this model. Scalapino and his collaborators^{16,17} proposed a diffusive instability toward the spatially inhomogeneous state by considering the quasiparticle density fluctuation effect within the μ^* model. Smith¹⁸ also discussed a diffusive instability in the two distinct gap states based on the physical arguments of quasiparticle distributions. Baru and Sukhanov¹⁹ studied an instability in

two different superconducting states, while Elesin²⁰ discussed the instability especially under electromagnetic irradiation.

In this paper, we report a quasiparticle injection experiment on aluminum films using Pb/Bi-I-Al-I-Al double-tunnel junctions which is similar to those by DNG and GW, but differs from them in the crucial respect that all three films had different gaps. Also, our injection voltages were extended well above the gap voltage so that quasiparticle injection was uniform over the injected superconducting film. As a result, we observe an intrinsic instability toward the spatially inhomogeneous state and fully developed multiple-gap states for injection above the gap-sum voltage.²⁵ The phenomena cannot be explained by the idea of inhomogeneous quasiparticle injection.^{13,14} We establish a theoretical model on diffusive quasiparticle instabilities which can account for our observations. We also confirm the two-gap states for injection at the gap-sum voltage, which represents only a special case within our model.

II. INSTABILITY MODEL

In this section, we study the instability which is induced under high quasiparticle injection within the framework of the μ^* model and follow the treatment by Scalapino and Huberman.¹⁷ According to the μ^* model, the instability arises as a consequence of the fact that a decrease of the effective chemical potential μ^* occurs for the quasiparticle concentration exceeding a certain critical concentration N_c because of rapid gap reduction due to high quasiparticle injection.

We begin with the phenomenological energy-independent Rothwarf-Taylor equations²⁶ modified to include quasiparticle diffusion

$$\frac{\partial N}{\partial t} = I_{qp} - 2RN^2 + \frac{2}{\tau_B} N_{ph} - \nabla \cdot \bar{J}, \quad (1)$$

$$\frac{\partial N_{ph}}{\partial t} = I_{ph} + RN^2 - \frac{1}{\tau_B} N_{ph} - \frac{N_{ph} - N_{ph}^T}{\tau_{es}}. \quad (2)$$

Here N and N_{ph} are the quasiparticle and phonon concentrations, respectively, and N_{ph}^T is the thermal equilibrium phonon concentration. I_{qp} and I_{ph} are, respectively, the quasiparticle and phonon injection rates, assumed uniform across the film interfaces. R is the quasiparticle recombination coefficient, τ_B is the phonon pair-breaking time, and τ_{es} is the phonon escape time. \bar{J} is the quasiparticle diffusion current density. In the steady state, the solution of Eqs. (1) and (2) becomes

$$N^2 = N_T^2 + (I_0 - \nabla \cdot \bar{J}) \frac{P}{2R}, \quad (3)$$

$$I_0 \equiv I_{qp} + \frac{2(P-1)}{P} I_{ph},$$

where $P \equiv 1 + \tau_{es}/\tau_B$ is the so-called phonon trapping factor and N_T is the thermal equilibrium quasiparticle concentration which satisfies the relation $N_{ph}^T/N_T^2 = R\tau_B$.

We assume that \bar{J} is given by the Scalapino-Huberman expression¹⁷

$$\bar{J} = -\frac{2D}{N(0)\Delta_0} (N_c - N) \nabla N + \frac{D\xi^2}{2} \nabla (\nabla^2 N), \quad (4)$$

where D is the quasiparticle diffusion constant, $N(0)$ is the Bloch single-spin density of states at the Fermi surface, Δ_0 is the zero-temperature equilibrium gap parameter, and ξ is the zero-temperature coherence length. The coefficient of the first term is negative when $N < N_c$, but positive when $N > N_c$. This effect is the key to the occurrence of a diffusive quasiparticle instability because it leads to quasiparticle diffusion from regions of low concentration to regions of high concentration when $N > N_c$. The second term acts to oppose rapid spatial changes due to the first term and stabilizes the spatial variation in N .

Combination of Eqs. (3) and (4) leads to a fourth-order nonlinear differential equation for N which precludes a simple analysis. Theoretically, however, it is possible to conjecture the fully developed nonlinear superconducting state. Huberman²⁷ obtained the numerical solution for the particle concentration in chemical reactions in the spinodal limit. The resultant distribution consisted of two regions within each of which the particle concentration is almost constant, with a narrow boundary region between them. Equation (3) with Eq. (4) has the same functional form as the case of chemical reactions. On the other hand, Smith¹⁸ obtained similar spatial structure for the gap parameter by physical arguments based on a diffusive instability. Experimentally, as shown in the next section, two or more distinct gap regions were observed, which suggests that the gap in each region is fairly constant. Therefore it seems reasonable to assume that in the fully developed multiple-gap state the quasiparticle concentration is constant within each region and has nonzero gradients only at the boundaries of the regions. We further assume that the normal component of the quasiparticle diffusion current density at the boundary s of such a region can be approximated by the first term of Eq. (4),

$$J_n = -\frac{2D}{N(0)\Delta_0} [N_c - N(s)] \left(\frac{\partial N}{\partial n} \right)_s, \quad (5)$$

where $(\partial N/\partial n)_s$ is the spatial gradient of N along the direction n in the plane of the film and normal to the boundary s . The stabilizing effect of the second term in Eq. (4) can be simulated by imposing some finite value on $(\partial N/\partial n)_s$. As shown later, $(\partial N/\partial n)_s$ is weakly dependent on I_0 compared with the factor $[N_c - N(s)]$, so that we can take it to be a constant without losing any essential features of the model.

With these assumptions, consider two distinct gap regions α and β at an injection rate above the threshold for the two-gap state. Integration of Eq. (3) with Eq. (4) over each region, using the divergence theorem of Gauss, yields

$$2R(N_\alpha^2 - N_f^2) = \hat{I}_0 - D_\alpha[N(s) - N_c] \quad (6)$$

$$2R(N_\beta^2 - N_f^2) = \hat{I}_0 + D_\beta[N(s) - N_c] \quad (7)$$

where $\hat{I}_0 \equiv PI_0$,

$$D_\alpha \equiv \frac{2DP}{N(0)\Delta_0} \left(\frac{L_s}{A_\alpha} \right) \left(\frac{\partial N}{\partial n} \right)_s,$$

and

$$D_\beta \equiv \frac{A_\alpha}{A_\beta} D_\alpha.$$

A_α and A_β are the areas of regions α and β , L_s is the perimeter of the boundary between the two regions, and the normal in $(\partial N/\partial n)_s$ is the outward normal from region α into region β . At the boundary we also have

$$2R[N^2(s) - N_f^2] = \hat{I}_0 \quad (8)$$

In principle, $N(s)$ should be obtained by solving the fourth-order differential equation. Elimination of $N(s)$ among Eqs. (6), (7), and (8) gives the equations for N_α and N_β

$$2R(N_\alpha^2 - N_c^2) = \hat{I}_0 - I_\beta + D_\alpha N_c - D_\alpha [N_c^2 + (2R)^{-1}(\hat{I}_0 - I_\beta)]^{1/2} \quad (9)$$

$$2R(N_\beta^2 - N_c^2) = \hat{I}_0 - I_\beta - D_\beta N_c + D_\beta [N_c^2 + (2R)^{-1}(\hat{I}_0 - I_\beta)]^{1/2} \quad (10)$$

where we have used the definition $I_\beta \equiv 2R(N_c^2 - N_f^2)$.

The behavior predicted by Eqs. (9) and (10) is shown schematically in Fig. 1. As the effective

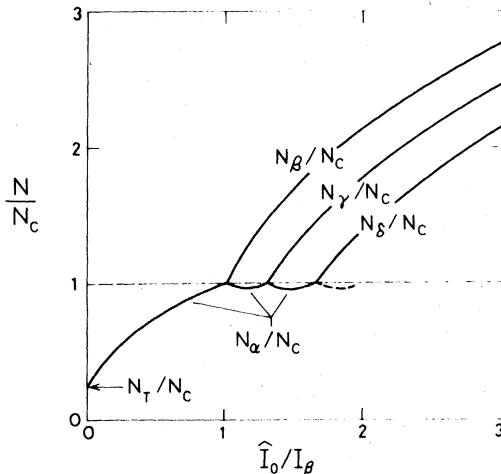


FIG. 1. Sample configuration.

quasiparticle injection rate \hat{I}_0 is increased from zero, N increases as $\hat{I}_0^{1/2}$ from N_f , as described by Eq. (3) with the diffusion term omitted because N is uniform throughout the film. When N reaches the critical concentration N_c , the quasiparticle concentration curve bifurcates as described by Eqs. (9) and (10). A high concentration (and hence low-gap) region β appears, within which the concentration increases (and the gap decreases) continuously as the injection rate is further increased. The concentration in the original α region first decreases slightly, then increases again. When it reaches N_c , a second bifurcation should occur, spawning a second high-concentration low-gap region, the γ region. The threshold for this second bifurcation is readily calculated, by setting $N_\alpha = N_c$, to be

$$\hat{I}_{0\gamma} = I_\beta + \frac{D_\alpha^2}{2R} - 2D_\alpha N_c \quad (11)$$

Similarly, the third bifurcation occurs at the injection rate

$$\hat{I}_{0\delta} = \hat{I}_{0\gamma} + \frac{E_\alpha^2}{2R} - 2E_\alpha N_c \quad (12)$$

where E_α is the same factor as D_α except that s refers to the boundary between the two regions α and γ . Within the model, such bifurcation may occur repeatedly.

Consequently at a series of threshold injection rates $\hat{I}_{0\delta} > \hat{I}_{0\gamma} > \hat{I}_{0\beta}$, we observe the appearance of superconducting regions with quite well-defined gaps $\Delta_{2\alpha} > \Delta_{2\delta} > \Delta_{2\gamma} > \Delta_{2\beta}$. Although in the model N_α remains essentially pinned at N_c above the first threshold, it does exhibit very small decreases between thresholds. The amount of decrease δN at the minimum point of the N_α curve is

$$\delta N = N_c \left[1 - \frac{[(1 + \sqrt{1+g})(3 - \sqrt{1+g})]^{1/2}}{2} \right] \quad (13)$$

where g is defined by $\hat{I}_{0\gamma} - I_\beta \equiv 2RN_c^2 g$. Numerical evaluation under the assumption of the linear dependence of gap parameter on quasiparticle concentration leads to the amount of the maximum gap enhancement in the region α to be $\delta\Delta = 0.74, 1.9,$ and $6.5 \mu\text{eV}$ for $g = 0.3, 0.5,$ and 1.0 , respectively, when $\Delta_0 = 300 \mu\text{eV}$.

Next we roughly evaluate the order of magnitude of the gradient $(\partial N/\partial n)_s$ at the boundary s from which the order of the boundary width is estimated. Since N_α is very close to N_c , Eqs. (6) and (8) lead to the approximate expression

$$\left(\frac{\partial N}{\partial n} \right)_s \approx \frac{2RN(0)\Delta_0 N_c A_\alpha}{DPL_s} \quad (14)$$

In general, $(\partial N/\partial n)_s$ is weakly dependent on the injection rate \hat{I}_0 . The magnitude of the recombination

coefficient R in Eq. (14) may be estimated from the equilibrium relation $R\tau_B = N_{\text{ph}}^T/N_f^T$ which has weak temperature dependence. In the limits $T \rightarrow 0$ and $T \rightarrow T_c$, we obtain

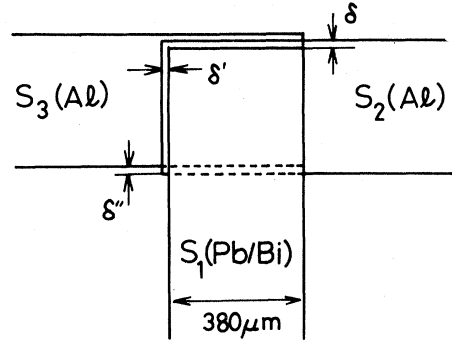
$$\begin{aligned} (R\tau_B)_{T=0} &= \frac{1}{4} \left(\frac{\Delta_0}{\pi \bar{c}_s \hbar} \right)^3 [N(0)\Delta_0]^2 \\ &= \frac{(2 \ln 2)^2}{\pi \zeta(3)} \left(\frac{\Delta_0}{k_B T_c} \right) (R\tau_B)_{T=T_c}, \end{aligned} \quad (15)$$

where $\zeta(3)$ is the Riemann ζ function and \bar{c}_s is the average sound velocity. For $\Delta_0 = 1.76 k_B T_c$, $(R\tau_B)_{T=0} \approx 0.9 (R\tau_B)_{T=T_c}$. Here we assume the value of R in the low-temperature limit. We also assume the relations $D = v_F d/3$ and $\tau_{\text{es}} = 4d/\eta \bar{c}_s$, where v_F is the Fermi velocity, d is the film thickness, and η is the average phonon-transmission probability at the film interfaces. For aluminum, a set of numerical values $v_F \approx 10^8$ cm/sec, $N(0) = 1.22 \times 10^{22}$ states/eV, $\Delta_0 = 0.3$ meV, $\tau_B = \tau_B(2\Delta_0) = 2.42 \times 10^{-10}$ sec,²⁸ $\bar{c}_s = 3.5 \times 10^5$ cm/sec, and $\eta = 0.5$ yields the phonon trapping factor $P \approx 1.5$ and $(\partial N/\partial n)_s \approx 3.3 \times 10^5 N_c (A_\alpha/L_s)$. It is interesting to note that $(\partial N/\partial n)_s$ depends only on the ratio A_α/L_s .

Suppose that the instability produces an alternating periodic pattern of regions α and β along the length of the film, which might be possible when the film width w is small compared to the length scale of the instability $2\pi/q_m$ given by the Scalapino-Huberman model. If l_α and l_β are the length of such regions α and β , respectively, we have $A_\alpha/L_s = l_\alpha$. The length scale of the fully developed nonlinear superconducting state is, however, unknown. For an order of magnitude estimate, we take $l_\alpha = 2\pi/q_m$, the value near the instability threshold. For aluminum, $2\pi/q_m = 30 \sim 60$ μm , which yields $(\partial N/\partial n)_s = (1 \sim 2) \times 10^3 N_c$ corresponding to the effective boundary width ξ_s of order of one micrometer. Therefore $2\pi/q_m$ is significantly greater than ξ_s , justifying our assumption of uniform quasiparticle concentrations within regions. Other possible structures such as a number of small regions β embedded in the α region background also yield the same order of magnitude of ξ_s .

III. SAMPLE PREPARATION

We used a S_1 -I- S_2 -I- S_3 double-tunnel-junction structure. S_1 was a Pb/Bi film, and S_2 and S_3 were Al films. The sample with its area 380×380 μm^2 was prepared by successive evaporation and oxidation of dirty Al and Pb/Bi films on a glass substrate. The oxidation of Al films was made by either glow discharge in a dry oxygen atmosphere or thermal oxidation in a wet oxygen atmosphere. The sample con-



$$\delta, \delta', \delta'' = 10 - 30 \mu\text{m}$$

FIG. 2. Schematic dependence of quasiparticle concentration on effective injection rate according to the model described in text.

figuration was illustrated in Fig. 2. The middle aluminum film S_2 was the thinnest ~ 500 \AA , while the bottom aluminum film which had contact with the substrate was about 1000 \AA . The S_1 -I- S_2 junction was used as an injector and had specific resistances ranging from 10^{-3} to 10^{-5} Ωcm^2 .

Because dirty aluminum films were used, it was possible to obtain films with different gap values by controlling evaporation conditions. In this experiment the gap parameter Δ_2 of film 2 was made appreciably smaller than Δ_3 of film 3. $\Delta_3 - \Delta_2$ ranged from 10 to 100 μeV among our samples. Typical values for the gap parameter Δ_1 and Δ_3 were 1.7 and 0.3 meV, respectively. The differences in materials, gap parameters, and thicknesses among the three films were designed to minimize nonequilibrium perturbations in films 1 and 3 due to pair breaking by recombination phonons diffusing throughout the sample structure. Hence the observed changes in the detector characteristics are considered to be nearly those of film 2 only. In this respect, our samples differ significantly from those of DNG¹² and GW.¹³ The three films in their samples were all of the same material and all three films were significantly perturbed by quasiparticle injection in their experiments.

The junction edges were not covered, but the junction films were carefully aligned to prevent direct tunneling between films 1 and 3 (see Fig. 2). In most samples the detector-junction area common to the injector was 90% or more of the total area. If the quasiparticle-diffusion effect is taken into account, we may consider that the nearly whole area of the detector film is exposed under quasiparticle injection. For the Pb/Bi injector junction, the $\Delta_1 - \Delta_2$ cusp was quite sharp and the negative resistance region was well defined. There was no detectable excess current and the current jump at the gap-sum voltage $(\Delta_1 + \Delta_2)/e$ was almost vertical (width ~ 25 μV). No

appreciable negative resistance was observed at the gap-sum voltage within the experimental error. The temperature dependence of the aluminum gap parameter Δ_2 was in excellent agreement with the prediction of the BCS theory and yielded $\Delta_{02}/k_B T_{c2} = 1.75 \pm 0.02$. In our experiments, the Pb/Bi-I-Al junctions proved to be of higher quality than the Al-I-Al junctions.

All measurements were performed with the sample immersed in superfluid helium for temperatures down to 1 K. The dc Josephson current was suppressed by applying a small parallel magnetic field.

IV. RESULTS AND DISCUSSION

For a given bias voltage of the injector junction, the detector I_d - V_d characteristic and its first derivative were measured. In all cases, it was observed that the energy gap of the middle aluminum film 2 first decreased uniformly with increasing injection current I_i . At a certain critical injection current $I_{i\beta}$, the instability toward the spatial inhomogeneous state occurred and the second gap region appeared. This threshold current $I_{i\beta}$ was approximately constant and found to be 5 ± 1 mA for injector specific resistance ranging over two orders of magnitude, so long as the sample was in direct contact with superfluid helium. The transition was continuous. For a relatively low-resistance injector, the instability occurred at the vertical rising portion of the injector characteristic, while for a relatively high-resistance injector, it occurred above the gap-sum voltage. A thin coating of photoresist film with thickness a few micrometers on the sample, which increases the phonon trapping factor, reduced the threshold value by several factors. A similar effect was also reported for Pb films.⁸ The subsequent behavior following the onset of the second gap region was qualitatively different between injection at the gap-sum voltage and above the gap-sum voltage. Physically, quasiparticle injection above the gap-sum voltage is considered to be uniform.

An example of our results for a relatively low-resistance injector is shown in Fig. 3. In this case, injection is dominantly held at the gap-sum voltage, hence the energy of the injected quasiparticles is Δ_2 . The effective injection rate \dot{I}_0 is proportional to injection current I_i and given by $\dot{I}_0 = PI_i/edA$ since $I_{ph} = 0$, where A is the film area exposed to quasiparticle injection.²⁹ As the injection current was increased, we first observed only a slight decrease in the gap-sum voltage in the detector current-voltage characteristic. Then, at point 2 on the injector characteristic there appeared a current rise in the detector characteristic at a voltage significantly below the original gap-sum voltage. The development of this voltage was rapid but not abrupt. From the threshold behavior in the dI_d/dV_d vs V_d characteristic, it was found that the

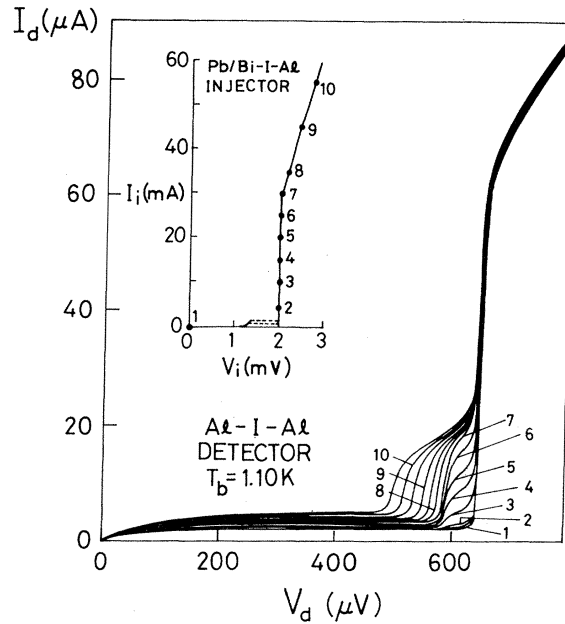


FIG. 3. Detector and injector (insert) current-voltage characteristics at $T_b = 1.10$ K. Detector-curve numbers correspond to indicated points on injector characteristic.

second gap region was continuously split off from the main first peak, although the detailed behavior close to the main peak was concealed by gap broadening. As the injection current was further increased, this rise grew in magnitude while remaining at the same voltage, until the injection current reached the top of the gap-sum step in the injector characteristic. Then the current rise appeared to saturate in magnitude but began to shift toward lower voltage. This behavior continued until either the injector-film critical current was reached or until the voltage at which the current rise occurred decreased to about half the original gap-sum voltage, depending on sample.

We interpret this behavior as indicating the nucleation and growth in film 2 of a region with a well-defined gap $\Delta_{2\beta}$ which is smaller than the gap $\Delta_{2\alpha}$ in the remainder of the film. As the injection current increases, $\Delta_{2\alpha}$ remains near the thermal-equilibrium gap of the film since no quasiparticle injection occurs in region α ; $\Delta_{2\beta}$ first remains relatively constant at a lower value while the size of the β region grows at the expense of the α region. This indicates that the injection rate per unit volume of regions β is fixed, the behavior expected from the free energy calculation. Then, after the injector current passes the top of the gap-sum step in the injector characteristic, $\Delta_{2\beta}$ decreases toward zero. The gradual decrease in the current height of $\Delta_{2\beta}$ above the gap-sum step injection has approximately a $(\Delta_{2\beta})^{1/2}$ dependence. This behavior is similar to that reported by DNG¹² and by GW.¹³ The phenomenon is, however, different from

those of DNG and GW in the fact that the threshold for the two-gap state occurred at different parts of the current jump in the injector characteristic depending on the magnitude of injector specific resistance, and that no hysteretic switching like that reported by DNG and by GW was found, although we did occasionally observe some indication of such switching in photoresist-coated samples. In addition, no appreciable negative resistance was recorded in the I_i - V_i characteristics of Pb/Bi-I-Al injector. If negative resistance would be essential for instability as suggested by GW, we would not expect different threshold values between the samples with and without photoresist coating. The gap difference $\Delta_{2\alpha} - \Delta_{2\beta}$ was also significantly increased by photoresist coating. The threshold current increased monotonically with increasing bath temperature.

Figure 4 shows temperature dependence of $\Delta_{2\alpha} - \Delta_{2\beta}$ at the gap-sum step injection. $\Delta_{2\alpha} - \Delta_{2\beta}$ decreased monotonically with increasing bath temperature. This behavior is of a puzzling nature because the equilibrium theory predicts just the opposite behavior, i.e., monotonical increase of $\Delta_{2\alpha} - \Delta_{2\beta}$ if both $\Delta_{2\alpha}$ and $\Delta_{2\beta}$ are assumed to have the BCS temperature dependence. The experimental data of $\Delta_{2\alpha}$ nearly obeys the BCS prediction, while that of $\Delta_{2\beta}$ deviates much from it and may be considered to be characteristic of the nonequilibrium instability. However, the situation given here, in which nonuniform injection occurs, represents a special case in our experiments.

Figures 5 and 6 show results for a higher resistance injector at different temperatures. For this sample, $\Delta_3 - \Delta_2 = 70 \mu\text{eV}$, and $\Delta_2 = 271 \mu\text{eV}$ at $T = 1.11 \text{ K}$, and $T_{c2} = 1.94 \text{ K}$. Here we observed no instability for injection currents on the gap-sum step in the injector characteristic. Rather, we observed for injection currents well above the gap-sum step the appearance of structures in the detector characteristic which we believe correspond to the nucleation and growth in

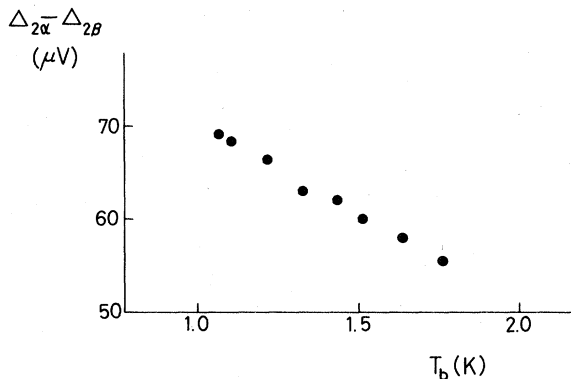


FIG. 4. Temperature dependence of gap parameter difference $\Delta_{2\alpha} - \Delta_{2\beta}$ in film 2 at gap-sum step injection.

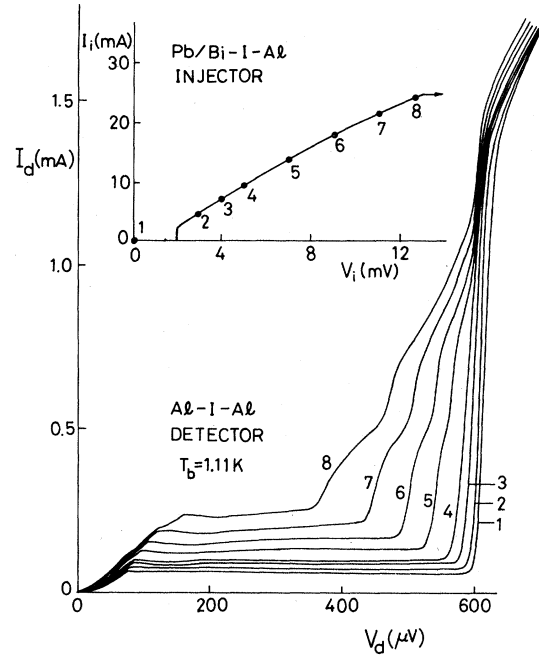


FIG. 5. Detector and injector (insert) current-voltage characteristics at $T_b = 1.11 \text{ K}$. Detector-curve numbers correspond to indicated points on injector characteristic.

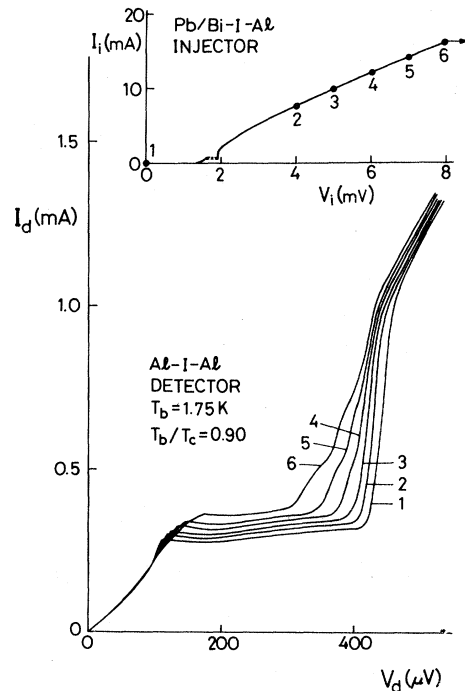


FIG. 6. Detector and injector (insert) current-voltage characteristics at $T_b = 1.75 \text{ K}$. Detector-curve numbers correspond to indicated points on injector characteristic.

film 2 of regions β with a reduced gap $\Delta_{2\beta}$, and of still further regions γ and δ with gaps $\Delta_{2\gamma}$ and $\Delta_{2\delta}$ intermediate in value between the "main" gap $\Delta_{2\alpha}$ and $\Delta_{2\beta}$. These new gaps are reflected in both the gap-sum and the gap-difference structures in the detector characteristic. They are of course more easily detected and followed in the first derivative of the detector characteristic. Figure 7 shows the dV_d/dI_d vs I_d characteristic for various values of the injection current I_i at $T = 1.1$ K. By measuring the corresponding peak heights in a dV_d/dI_d vs I_d curve as a function of injection current I_i and extrapolating to zero peak height, we found for the sample of Fig. 5 the following threshold currents for the appearance of the second-, third-, and fourth-gap regions: $I_{i\beta} = 6.4$ mA, $I_{i\gamma} = 8.1$ mA, and $I_{i\delta} = 10.7$ mA. The regions appeared continuously in second-order fashion and the corresponding gap-structure signals grew continuously in size with increasing injection current. The multiple-gap states were observed for all temperatures experimentally studied. It is interesting to point out here that all new regions β , γ , δ were split off from the main α region.

Temperature dependences of these threshold currents are qualitatively similar. All the threshold currents increased monotonically with increasing bath

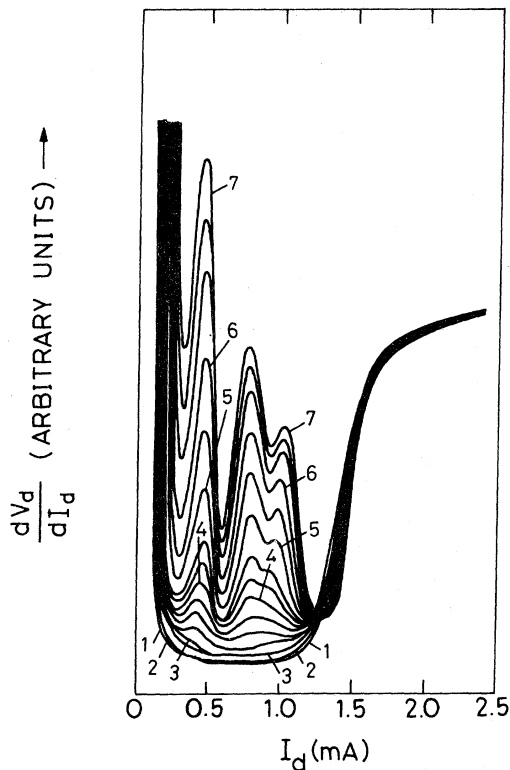


FIG. 7. Detector first derivative in voltage vs current characteristics. Detector-curve numbers correspond to indicated points on injector characteristic of Fig. 5.

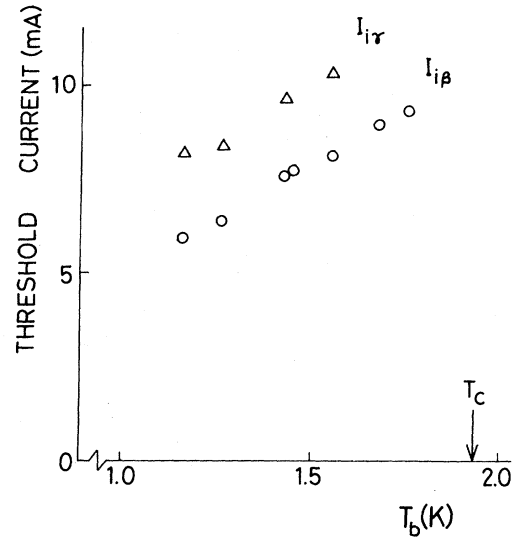


FIG. 8. Temperature dependence of instability-threshold currents.

temperature. An example of such dependence is shown in Fig. 8. Near $T = T_c$, however, the determinations of the threshold values became obscure since the whole structures including the derivative characteristics were smeared out.

Figure 9 shows the change of energy gaps as a function of injection current. $I_{i\beta}$, $I_{i\gamma}$, and $I_{i\delta}$ are the values determined by the first-derivative extrapolation method as stated above. It is clear to see that the uniform energy gap first decreases, then the in-

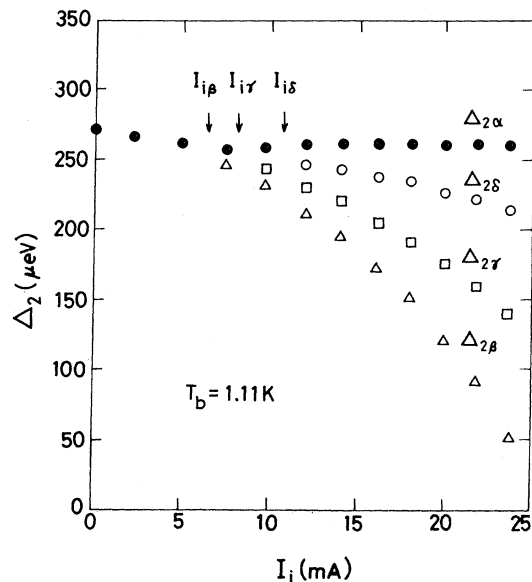


FIG. 9. Energy gap parameters in film 2 vs injection current at $T_b = 1.11$ K.

stability occurs, which leads to the subsequent appearance of the multiple-gap regions with $\Delta_{2\alpha} > \Delta_{2\delta} > \Delta_{2\gamma} > \Delta_{2\beta}$ at a series of threshold injection currents $I_{i\delta} > I_{i\gamma} > I_{i\beta}$. The smallest gap $\Delta_{2\beta}$ almost reaches zero at about $I_i = 25$ mA, indicating that the mixed state of superconducting and normal regions are possible for higher injection.

The results obtained experimentally are consistently explained if we assume the instability model developed in Sec. II. The relation between the effective injection rate \hat{I}_0 and injection current I_i for injection above the gap-sum voltage is different from that at the gap-sum voltage. For a bias voltage $V_i \geq (\Delta_1 + 3\Delta_2)/e$, the relaxation phonons with energy $\hbar\omega \geq 2\Delta_2$ also contribute to create excess quasiparticles by pair-breaking process [$I_{ph} \neq 0$ in Eq. (3)]. As shown experimentally later, the effect of I_{ph} gives an additional term to \hat{I}_0 which becomes proportional to I_i , not I_i^2 for an aluminum film. Therefore \hat{I}_0 has linear dependence on I_i . This fact supports our experimental fact that the threshold for the instability is determined by the injection current rather than the power dissipated.

Then the qualitative features of the appearance of superconducting regions with quite well-defined gaps $\Delta_{2\alpha} > \Delta_{2\delta} > \Delta_{2\gamma} > \Delta_{2\beta}$ are exactly those predicted in Sec. II. Although in the model N_α remains essentially pinned at N_c above the first threshold, it does exhibit very small decreases between thresholds as given in Eq. (13). In fact, we have experimentally observed a slight increase (≤ 5 μ V) in $\Delta_{2\alpha}$ above the first threshold which corresponds to the same order of magnitude as given by Eq. (13), consistent with this feature of the model. In the dI_d/dV_d vs V_d characteristic, this phenomenon appeared as the main gap peak at the gap-sum voltage first deformed and broadened, then its separation occurred, resulting in a slight enhancement of a higher gap.

At the third gap threshold $\hat{I}_0 = \hat{I}_{0\gamma}$, the quasiparticle concentrations at the boundary $N(s)$ and in the β region N_β are given by $N_c\sqrt{1+g}$ and $N_c[1+g \times (1+A_\alpha/A_\beta)]^{1/2}$, respectively, according to Eqs. (7) and (8). The measurements showed $I_{i\gamma} \sim 1.3 I_{i\beta}$ for the sample of Fig. 5, hence $g \sim 0.3$, which results in $N(s) \sim 1.1N_c$ and $N_\beta \sim 1.4N_c$ for $A_\alpha/A_\beta = 2$. The experimental structures in the detector characteristics are clearly more smeared than the original unperturbed gaps, indicating that the gap in the reduced-gap regions is not strictly constant, which allows a diffusion of quasiparticles. Nevertheless, the structures suggest that the spatial variation within each reduced-gap region is relatively small, as is also theoretically suggested in other circumstances.

The temperature dependence of the third gap threshold in Fig. 8 is consistent with this model since the second and third terms of the right-hand side of Eq. (11) are only weakly dependent on temperature. The threshold quasiparticle concentration N_c is es-

timated from the observed values of $I_{i\beta}$ to be 10^{17} – 10^{18} cm^{-3} , which significantly depends on the values of the parameters used such as the recombination coefficient, phonon trapping factor, electronic density of states, etc. The observed differences in threshold current between samples with and without photoresist coating is also consistent with the model since \hat{I}_0 differs from I_0 by a phonon trapping factor P . Furthermore, the larger A_β means a higher $I_{i\gamma}$, hence making observations of the third-gap state more difficult. In fact, we have observed the third-gap state mostly when $A_\alpha/A_\beta > 2$. The ratio A_α/A_β is estimated from the experimental data on current jump height. Approximately two-thirds of our samples showed as many as three distinct reduced gaps. Equation (14) suggests that the boundary width ξ_s is proportional to the phonon trapping factor P . In photoresist-coated samples, we have observed greater smearing of the gap structure which qualitatively agrees with the behavior predicted by Eq. (14).

The existence of the multiple-gap states is based on uniform injection. The absence of the third- and fourth-gap states for injection at the gap edge in our experiments is consistent with the model. Note that Eqs. (6) and (7) do not hold any more for nonuniform injection at the gap-sum voltage.

We have also performed the experiment using the same type of double-tunnel junction but in an opposite tunnel resistance configuration so that the Al-I-Al junction may serve as an injector and the Pb/Bi-I-Al junction as a detector. The distinct gap structure again appeared in the I_d - V_d characteristic of the Pb/Bi-I-Al junction. The appearance of the two-gap state qualitatively differs from the recent observations by Willemsen and Gray.³⁰

In order to study the phonon contribution I_{ph} due to relaxation of the injected quasiparticles for bias voltages $V_i \geq (\Delta_1 + 3\Delta_2)/e$, we performed an experiment in analogy with the phonon transfer experiments^{31,32} but using our double-tunnel-junction configuration. By biasing the detector junction at a voltage $V_d < (\Delta_2 + \Delta_3)/e$, the detector response signal was taken as a function of injection I_i or bias voltage V_i . In this case, the detector signal gives a measure of the number of excited quasiparticles in film 2. Figure 10 shows such a result. At $V_i = (\Delta_1 + 3\Delta_2)/e$ well below the instability threshold, we observed a sharp kink in detector signal. At this point Δ_2 was reduced uniformly by several μ V. This gradient discontinuity appeared as a result of the onset of an additional increase in quasiparticle concentration due to the pair breaking by additional phonons with $\hbar\omega \geq 2\Delta_2$ produced by relaxation of high-energy quasiparticles. For higher voltages, however, no clear structure could be seen and behavior was approximately linear. Note that $I_{i\beta}$ was about 5 mA. Consequently we conclude that the phonon injection rate I_{ph} for bias voltages $V_i \geq (\Delta_1 + 3\Delta_2)/e$ becomes pro-

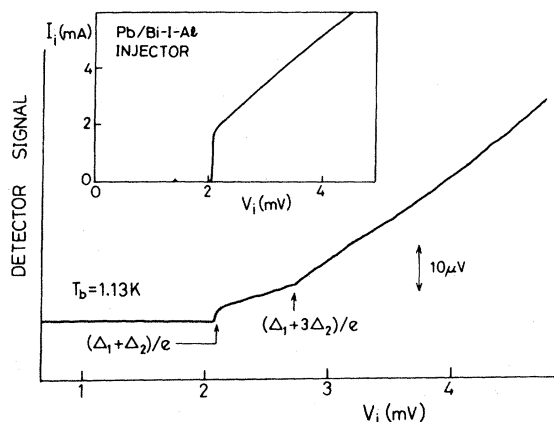


FIG. 10. Detector signal vs injector bias voltage. The inset shows injector characteristic.

portional to injection current I_i . Previous measurements on phonon transmission suggest the emitted phonon spectrum which extends from zero energy to an intense peak at $2\Delta_2$ followed by a rapidly decaying tail for higher energies.³¹ If this would be the case, the phonon pair-breaking effect in film 1 due to the emitted phonons from film 2 would be considerably reduced when Δ_1 is slightly higher than Δ_2 . This is exactly the fact we found in our experiments.

In our model, in order to realize the well-defined multiple-gap states, we have to choose such a sample material that the relation $2\pi/q_m \gg \xi_s$ should be satisfied and its sample size L should be significantly greater than $2\pi/q_m$. For a sample with its dimension $L < 2\pi/q_m$, the instability toward the spatially inhomogeneous state will not occur and a uniform transition will be expected. Both $2\pi/q_m$ and ξ_s depend on the film thickness d and the phonon transmission probability η . As a consequence, it is important to reduce the phonon trapping factor P for observation of distinct gap states. This can be achieved by taking a thinner film and better acoustical matching to the adjacent substrate or liquid helium.

In case of a lead film, the phonon trapping factor is large and about 50 for film thickness of 1000 Å. The length scale of the instability $2\pi/q_m$ is small (order of a few μm) because of the much shorter recombination time and coherence length than aluminum. The above facts contribute to make the gradient $(\partial N/\partial n)_s$ relatively smaller, hence the boundary width ξ_s larger. The calculated ξ_s for a Pb film of thickness 1000 Å is about 5 μm . Then, it is easy to conjecture smearing of gap structures in the detector characteristics.³³ In the case of tin, the corresponding

situation lies somewhere between those of Pb and Al. The phonon trapping factor for tin is usually 10–20 and $2\pi/q_m$ is about 10 μm for film thickness 1000 Å.¹⁷ The above arguments might be applicable only near the instability threshold, since the length scale of the well-developed nonlinear distinct-gap state is unknown.

V. CONCLUDING REMARKS

We have experimentally shown the occurrence of an intrinsic instability due to quasiparticle injection through a tunnel barrier and the appearance of fully developed well-defined multiple-gap states. The results were consistently interpreted by the μ^* instability model in spite of our crude treatment. It was shown that, while the instability toward the two-gap state occurred either at the gap-sum voltage or above the gap-sum voltage of the injector characteristic according as the magnitude of tunnel resistance, the third- and fourth-gap states were only observable for injection above the gap-sum voltage whose situation corresponds to uniform injection of quasiparticles into a superconducting film.

The threshold current density was nearly constant $\sim 3.5 \text{ A/cm}^2$ for injector specific resistances ranging over two orders of magnitude and the transition occurred in a second-order fashion. The results were qualitatively different from those reported in the previous measurements^{12,13} even for the case in which only a two-gap state was involved. Our phenomena cannot be explained by the load-line switching model based on nucleation of small spatial inhomogeneities in a film.^{13,14} Although the qualitative features of the experimental data agree with the μ^* instability model, it is more important to find out the shape of quasiparticle distribution experimentally than to make a detailed comparison with the μ^* model. We have also reported that lots of properties of the nonequilibrium state were affected by a coating of photoresist on sample surface, reflecting the fact that various nonequilibrium states are possible depending on the sample surroundings.⁸

We have assumed that this state is time independent. We have no experimental evidence to the contrary. In light of recent developments in understanding of nonequilibrium hydrodynamic instabilities (e.g., the Rayleigh-Bernard instability), it is interesting to speculate on the possible similarities between such phenomena in fluids and superconductors in particular whether time-dependent spatially inhomogeneous nonequilibrium superconducting states may also exist under appropriate circumstances.

- ¹See, for example, I. Prigogine, G. Nicolis, and A. Babloyantz, *Phys. Today* **25**, 23 (1972); H. L. Swinney and J. P. Gollub, *ibid.* **31**, 41 (1978).
- ²G. A. Sai-Halasz, C. C. Chi, A. Denenstein, and D. N. Langenberg, *Phys. Rev. Lett.* **33**, 215 (1974).
- ³P. Hu, R. C. Dynes, and V. Narayanamurti, *Phys. Rev. B* **10**, 2786 (1974).
- ⁴J. Fuchs, P. W. Epperlein, M. Welte, and W. Eisenmenger, *Phys. Rev. Lett.* **38**, 919 (1977).
- ⁵L. R. Testardi, *Phys. Rev. B* **4**, 2189 (1971).
- ⁶A. I. Golovashkin, K. V. Mitsen, and G. P. Motulevich, *Zh. Eksp. Teor. Fiz.* **68**, 1408 (1975) [*Sov. Phys. JETP* **41**, 701 (1976)].
- ⁷I. Iguchi, *Phys. Rev. B* **16**, 1954 (1977).
- ⁸I. Iguchi, *J. Low Temp. Phys.* **31**, 605 (1978); **33**, 439 (1978).
- ⁹I. Iguchi, *Phys. Lett.* **64A**, 415 (1978).
- ¹⁰G. Dharmadurai and B. A. Ratnam, *Phys. Rev. B* **20**, 4633 (1979).
- ¹¹R. Janik, L. Morelli, N. C. Cirillo, Jr., J. N. Lechevet, and W. D. Gregory, *IEEE Trans. Mag.* **MAG-11**, 687 (1975).
- ¹²R. C. Dynes, V. Narayanamurti, and J. P. Garno, *Phys. Rev. Lett.* **39**, 229 (1977).
- ¹³K. E. Gray and H. W. Willemsen, *J. Low Temp. Phys.* **31**, 911 (1978).
- ¹⁴K. Hida, *Phys. Lett.* **68A**, 71 (1978).
- ¹⁵C. S. Owen and D. J. Scalapino, *Phys. Rev. Lett.* **28**, 1559 (1972).
- ¹⁶J. -J. Chang and D. J. Scalapino, *Phys. Rev. B* **10**, 4047 (1974).
- ¹⁷D. J. Scalapino and B. A. Huberman, *Phys. Rev. Lett.* **39**, 1365 (1977); see also K. Hida, *J. Low Temp. Phys.* **32**, 881 (1978).
- ¹⁸L. N. Smith, *J. Low Temp. Phys.* **28**, 519 (1977).
- ¹⁹V. G. Baru and A. A. Sukhanov, *Zh. Eksp. Teor. Fiz., Pis'ma* **21**, 209 (1975) [*Sov. Phys. JETP Lett.* **21**, 93 (1975)].
- ²⁰V. F. Elesin, *Zh. Eksp. Teor. Fiz.* **71**, 1490 (1976); **73**, 355 (1977) [*Sov. Phys. JETP* **44**, 780 (1976); **46**, 185 (1977)].
- ²¹A. G. Aronov and B. Z. Spivak, *Fiz. Nizk. Temp.* **4**, 1365 (1978) [*Sov. J. Low Temp. Phys.* **4**, 641 (1978)], and the references therein.
- ²²U. Eckern, A. Schmid, M. Schmutz, and G. Schön, *J. Low Temp. Phys.* **36**, 643 (1979).
- ²³G. Schön and A.-M. Tremblay, *Phys. Rev. Lett.* **42**, 1086 (1979); A.-M. Tremblay and G. Schön (unpublished).
- ²⁴S. Imai, *J. Low Temp. Phys.* **40**, 595 (1980).
- ²⁵I. Iguchi and D. N. Langenberg, *Phys. Rev. Lett.* **44**, 486 (1980).
- ²⁶A. Rothwarf and B. N. Taylor, *Phys. Rev. Lett.* **19**, 27 (1967).
- ²⁷B. A. Huberman, *J. Chem. Phys.* **65**, 2013 (1976).
- ²⁸S. B. Kaplan, C. C. Chi, D. N. Langenberg, J. -J. Chang, S. Jafarey, and D. J. Scalapino, *Phys. Rev. B* **14**, 4854 (1976).
- ²⁹In Ref. 25, we incorrectly stated " N increases from N_T , linearly at first" at the 11th line of the right column of p. 488, which should be corrected as " N increases as $t_i^{1/2}$ from N_T ."
- ³⁰H. W. Willemsen and K. Gray, *Phys. Rev. Lett.* **41**, 812 (1978).
- ³¹A. H. Dayem and J. J. Wiegand, *Phys. Rev. B* **5**, 4390 (1972); A. H. Dayem, B. I. Miller, and J. J. Wiegand, *ibid.* **3**, 2949 (1971).
- ³²A. R. Long and C. J. Adkins, *Philos. Mag.* **27**, 865 (1973).
- ³³Very recently, H. Akoh and K. Kajimura reported the observation of the two-gap state for injection above the gap-sum voltage in Pb film, although the observed structures are considerably smeared out [Japan Physics Society Meeting, October, 1980 (unpublished)].